Princeton Plasma Physics Laboratory

PPPL- 4519

PPPL- 4519

Development of a Spatially Resolving X-Ray Crystal Spectrometer (XCS) for Measurement of Ion-Temperature (Ti) and Rotation-Velocity (v) Profiles in ITER

K. W. Hill, M. Bitter, L. Delgado-Aparicio, D. Johnson, R. Feder, P. Beiersdorfer, J.Dunn, K. Morris, E. Wang, M. Reinke, Y. Podpaly, J. E. Rice, R. Barnsley, M. O'Mullane, and S. G. Lee

May, 2010

Prepared for the U.S. Department of Energy under Contract DE-AC02-09CH11466.

Development of a Spatially Resolving X-Ray Crystal Spectrometer (XCS) for Measurement of Ion-Temperature (T_i) and Rotation-Velocity (v) Profiles in ITER[a)]

K. W. Hill,[1,b)] M. Bitter,[1] L. Delgado-Aparicio,[1] D. Johnson,[1] R. Feder,[1] P. Beiersdorfer,[2] J. Dunn,[2] K. Morris,[2] E. Wang,[2] M. Reinke,[3] Y. Podpaly,[3] J. E. Rice,[3] R. Barnsley,[4] M. O'Mullane,[5] and S. G. Lee[6]

[1]*PPPL, Princeton, NJ 08543, USA*
[2]*LLNL, Livermore, CA 94550, USA*
[3]*MIT-PSFC, Cambridge, MA 02139, USA*
[4]*ITER, Cadarache Centre, France*
[5]*Univ. Strathclyde, Glasgow, G4 0NG, UK*
[6]*NFRC, KBSI, Daejeon, Korea*

Imaging XCS arrays are being developed as a US-ITER activity for Doppler measurement of T_i and v profiles of impurities (W, Kr, Fe) with ~7 cm (a/30) and 10-100 ms resolution in ITER. The imaging XCS, modeled after a PPPL-MIT instrument on Alcator C-Mod, uses a spherically bent crystal and 2d x-ray detectors to achieve high spectral resolving power (E/dE>6000) horizontally and spatial imaging vertically. Two arrays will measure T_i and both poloidal and toroidal rotation velocity profiles. Measurement of many spatial chords permits tomographic inversion for inference of local parameters. The instrument design, predictions of performance, and results from C-Mod will be presented.

I. Introduction

A spatially resolving or 1d imaging x-ray crystal spectrometer (XCS) array is being designed to measure profiles of T_i, T_e, and plasma flow velocities on the International Tokamak Experimental Reactor (ITER).[1] This diagnostic is informed from prototype instruments already operating or to be installed on existing tokamaks throughout the world.[2,3] Favorable characteristics of this diagnostic are that it is very simple in structure, one instrument can measure the entire plasma profile, or a large fraction thereof, the spectrometer can continue taking data for long duration pulses, and it does not need neutral beam injection to operate. In this paper we highlight the status of the instrument design and present some simulations of the expected temporal and spatial resolution of the measurements of T_i and v.

The imaging XCS diagnostic has been described in detail previously,[2,3,4,5] and will only be briefly discussed here. It uses a spherically bent crystal to both disperse and image x rays emitted from the plasma onto a two-dimension detector. This paper will focus on factors which will determine the expected performance of the ITER core imaging x-ray spectrometer (CIXS).

II. Status of Instrument Design

The spectrometer will be housed inside ITER equatorial port #9 as illustrated in Fig. 1. In order to measure x rays from the upper half of the ITER plasma cross section, two spherical crystals and associated arrays of imaging detectors will be used. This configuration will be replicated, with one spectrometer version

[a)] Contributed paper published as part of the Proceedings of the 18th Topical Conference on High-Temperature Plasma Diagnostics, Wildwood, New Jersey, May, 2010.
[b)] Author to whom correspondence should be addressed. Electonic mail: khill@pppl.gov.

viewing radially inward toward the tokamak center, and the second instrument rotated ~10° about a vertical axis in order to view the plasma with a ~25% tangential component. The first spectrometer will measure T_i and poloidal flow velocities, and the second will measure T_i and toroidal flow velocities.

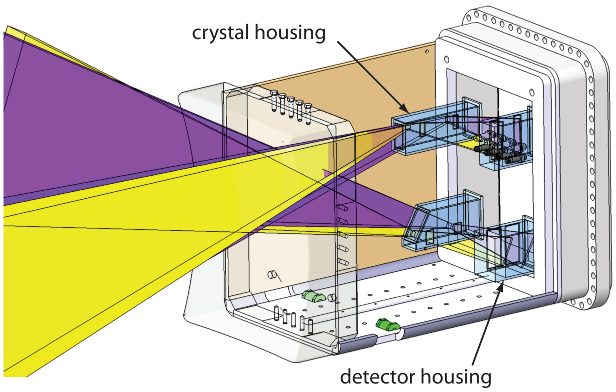

Fig. 1 Illustration of crystals and detectors inside individual secondary vacuum housings within the equatorial #9 port plug. The ITER plasma is to the left.

III. Simulations of Performance

Several factors contribute to or effect the performance. First, the spectrometer must have sufficient wavelength resolution to effectively measure the small Doppler induced changes in line position and width from which the flow v and Ti are inferred. Secondly, the emission line must be sufficiently bright to enable enough photon counts to be collected from sufficiently small regions (chords) of the plasma in the desired time period. That is, the statistical uncertainties must be sufficiently small. Thirdly other factors, which may degrade the measurement, such as instrumental or detector variations in efficiency, background counts from nuclear radiation or x-ray continuum, or tomographic inversion effects, must be minimally perturbing.

A. Simulation of X-Ray Brightness

For the highest power phase of ITER operation, L-shell transitions of Ne-like W at x-ray energies near 8.3 and 9.1 keV have been identified as favorable for Doppler measurements.[1] Tungsten will be an indigenous impurity in ITER, as it is a component of the first wall, and, thus, will not have to be artificially introduced into the plasma; the ionization potential of Ne-like W is sufficiently high that this charge state will exist over the electron-temperature (T_e) range 10-30 keV; and the x-ray energies are in a region for which diffracting crystals with reasonably good reflectivity can be found.

Simulations of Ne-like W L-line brightness profiles were done, and an IDL code was developed to tomographically invert the "measured" brightnesses in order to infer the local emissivity, T_i, and v_{tor}.

The SANCO impurity transport code was used to simulate the charge-state distribution and Ne-like W L-shell line emissivity for the ITER "scenario 2" H-mode plasma discharge.[6] Atomic data for the simulations were derived from ADAS.[78] This discharge has a centrally peaked Te profile with maximum value of 24 keV, and a flat density profile with core density of 10^{20} electrons/cm^3. The W concentration was assumed to be 10^{-5} relative to the electron density. The peak emissivity of the 9.1 keV W L line is about 1.5×10^{11} photons/cm^3/s. An array of spectrometer sightlines was generated, and the W line emissivity was integrated along the sightlines to simulate the line-brightness profile measured by the spectrometer. Then the diffracted intensity of these lines from a crystal having an area of 50 cm^2 and an integrated reflectivity of 20 mrad was calculated to provide an estimate of the count rate from each spatial resolution element of the plasma.

The main parameter inferred from the simulation of line brightness and transmission through the spectrometer to the detector was a count rate vs. radial position, which provides information on the statistical uncertainty of the values of T_i and v_{tor} which can inferred from the spectral lines. The ITER specifications call for measurement of T_i in 100 ms with 10% uncertainty and measurement of vtor in 10 ms with 30% uncertainty. For this simulation a count rate greater than 10^5 could be obtained for a viewing chords up to about 200 cm above the midplane or a normalized minor radius near 0.73. Thus, the statistical contributions to the uncertainty in T_i and v_{tor} would satisfy the ITER specifications up to this minor radius for the simulation conditions above. To make measurements further out in minor radius, lower Z ions, such as Fe should be used.

B. Determination of T_i and v_{tor} from X-Ray Spectra

In addition, at each point along the sightlines a Doppler shifted and broadened Gaussian line profile, weighted by the local emissivity, was generated at each point. For this simulation, the toroidal rotation velocity profile was chosen to be proportional to the T_e profile; the T_e profile was truncated at 10 keV, and normalized to 100 km/s. This synthetic spectrum was integrated along each sightline to provide the spectral brightness, and this chordally integrated spectral line was fitted with a Gaussian function in order to infer the "apparent" or non-inverted T_i and v_{tor} for that sightline. These apparent values are shown in Fig. 1 as the blue curves. The black curves represent the local values. These comparisons show that the un-inverted parameters inferred from the line-integrated spectra differ by less than 25% from the true local values.

C. Tomographic Inversion of Simulated Spectra

The analysis of Condrea *et al.*[9] was used to perform a tomographic inversion of the simulated spectral brightnesses in order to reconstruct the local emissivity, T_i, and v_{tor}. Concentric zones of constant poloidal flux were generated with flux values defined by those values at the points of tangency of the sightlines with the flux surfaces. Then Condrea's L_{ij} matrix elements were calculated geometrically as the path lengths within zone i of the j-th sightline, and the associated $\cos q_{ij}$ values, where q_{ij} is the angle between the j-th line of sight and the local vtor in zone i, were determined.

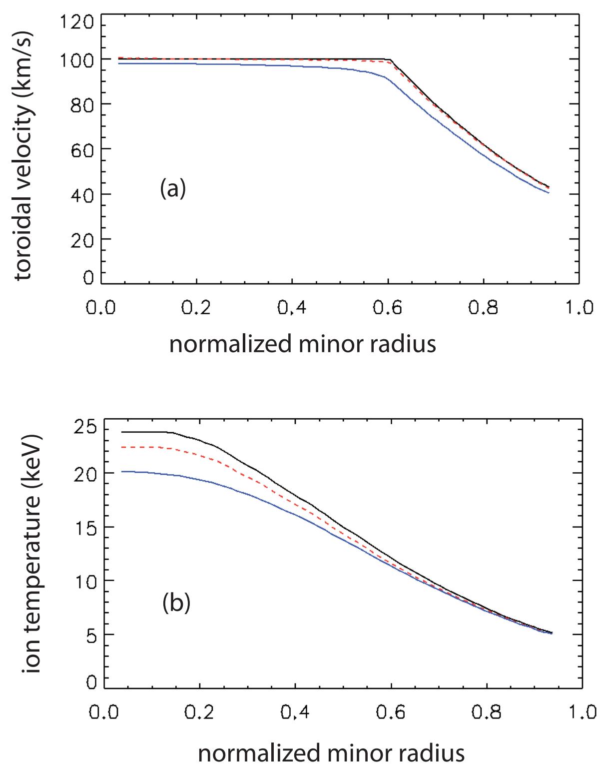

Fig. 2 Plasma toroidal flow velocity and (b) ion temperature vs. normalized minor radius for ITER scenario 2 H-mode discharge. Curves shown are local values (black, solid), inferred from Gaussian fits to chordally integrated spectra (blue solid), and inverted from chordally integrated fits (red dashed).

A comparison of the reconstructed local T_i and v_{tor} profiles with both the actual local values and the non-inverted values is shown in Fig. 2 for the spectrometer that can measure a component of v_{tor}. We can see that the reconstruction of the v_{tor} profile is almost perfect, and the inverted T_i profile differs from the local values by less than 7%. For the strictly radially viewing spectrometer, the reconstructed central T_i is only 4% less than the local value. The discrepancy between the "local" T_i values along the sightlines and the reconstructed T_i values is believed to be due partially to the fact that the simulated "data" used for the inversion did not satisfy the assumptions of the inversion equations, namely that the relevant plasma parameters (T_i and emissivity) be constant on flux surfaces. Work is in progress to replace the non-constant values on each flux surface with the poloidal average value, in order to see if the local T_i values can be reconstructed from the chordal averages by the inversion. Another possibility for the small discrepancy is that the actual profiles of the line-integrated spectra have a different shape than the fitted Gaussian line profiles which were used to infer the T_i values.

D. Effect of Background Noise on Measurements

The detectors will have a uniformly distributed background count rate due to both x-ray continuum diffracted from the crystal, and noise counts due to the ambient fusion nuclear radiation which cannot be completely shielded out. An analysis of the contribution of this background to the uncertainty in measurement of T_i and v_{tor} has been presented previously. As an example, the uncertainty in the measurement of the line position, or vtor, will be increased by a factor of 2 for a background level equal to the height of the spectral line. The uncertainty in measurement of the line width will be increased by a factor of 3 for this same background level. Thus the uncertainty in T_i would be increased by a factor of 6, since $T_i \sim\sigma^2$, where σ is the width parameter of the spectral line's Gaussian distribution. Thus an estimate of both the continuum background and a careful neutronics analysis needs to be done in order to refine the present estimates of performance.

IV. Reduction of Nuclear Radiation Background by Pulse Height Discrimination

Recent measurements on NSTX of the signals generated in a Pilatus II detector by the fusion neutrons and secondary gamma rays suggest that excellent discrimination against this nuclear background can be achieved by selection of a pulse-height window encompassing the narrow spectral band ($\Delta E/E \sim 0.01$) used to make the Doppler measurements. The detectors being used on the C-Mod imaging XCS are Pilatus100k sensors.[10] These devices are pixel array sensors having 487 x 195 individual x-ray photon counting detectors of size 0.172x0.172 mm^2. Each pixel of the Pilatus II detector has only a single, lower level discriminator (LLD), used for rejection of electronic noise and fluorescence background. The total nuclear generated background counts in all ~95,000 pixels of a Pilatus II detector were measured for different LLD settings ranging from 2 to 30 keV during several NSTX discharges. These data were then normalized to the total number of neutrons generated during each discharge. The resulting spectrum of counts/neutron vs. energy threshold are shown in Fig. 3

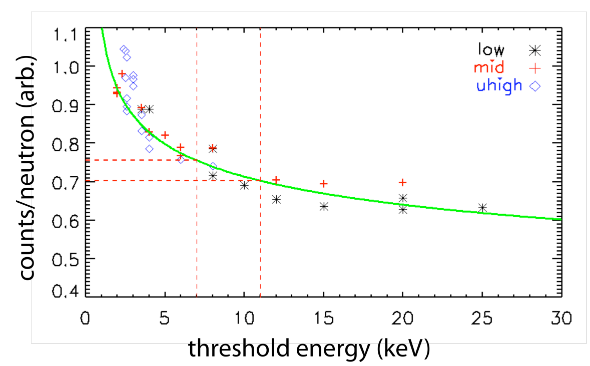

Fig. 3 Counts in a Pilatus 100k detector due to fusion nuclear radiation, normalized to the total number of NSTX neutrons, vs. Pilatus energy threshold setting for low, mid, and ultra high amplifier gain settings.

The solid curve is a power law with exponent -0.150. The data show that a single LLD set to ~7 keV (for detection of 9 keV x rays) discriminates against only ~ 25% of the nuclear background. If, however, an additional upper level discriminator (ULD) set to ~ 11 keV is used, more than 90% of the nuclear background can be rejected. Since the width of the Pilatus pulse-height distribution is of order 500 eV FWHM, this ~ 4 keV wide window should accept > 95% of the x rays. Since, even with maximum nuclear shielding, the detector environment around ITER can be expected to have relatively high levels of nuclear radiation, it is important to encourage the pixel array detector developers to include both LLDs and ULDs in their electronics. The current Pilatus II detectors and the faster framing Eiger detectors have only a single LLD. Each pixel of the Medipix II chip, however, has both a LLD and a ULD. It is anticipated that a future upgrade of Pilatus will also have an ULD.

V. Acknowledgements

This work is supported by the US Department of Energy under contract DE-ACO2-76-CHO-3073.

VI. References

[1] P. Beiersdorfer, J. Clementson, J. Dunn, M. F. Gu, K. Morris,
Y. Podpaly, E. Wang, M. Bitter, R. Feder, K. W. Hill, D. Johnson
and R. Barnsley, J. Phys. B:At. Mol. Opt. Phys. **43**, 1 (2010) (in press)

[2] Bitter, RSI99 (NSTX)

[3] A Ince-Cushman, J.E. Rice, M. Bitter, M.L. Reinke, K.W. Hill, M.F. Gu, E. Eikenberry, Ch. Broennimann, S.G. Lee, Y. Podpaly, Rev. Sci. Instrum. **79**, 10E302 (2008).

[4] M. Bitter, K. W. Hill, B. Stratton, A. L. Roquemore, D. Mastrovito, S. G.
Lee, J. G. Bak, M. K. Moon, U. W. Nam, G. Smith et al., Rev. Sci.
Instrum. **75**, 3660 (2004).

[5] K.W. Hill, M.L. Bitter, S.D. Scott, A. Ince-Cushman, M. Reinke, J.E. Rice, P. Beiersdorfer, M-F Gu, S.G. Lee, Ch. Broennimann, and E.F. Eikenberry, Rev. Sci. Instrum. **70**, 10E320 (2008).

[6] M. Shimada, Plasma Performance Assessment—August
2004, ITER report 27SZNW v1.0

[7] H. P. Summers, The ADAS User Manual—version 2.7 University of
Strathclyde, Glasgow, (2004), http://adas.phys.strath.ac.uk

[8] H. P. Summers et al., Plasma Phys. Controlled Fusion **48**, 263 (2006).

[9] I. Condrea, E. Haddad, B. C. Gregory, and G. Abel, Phys. Plasmas **7**, 3641
(2000).

[10] Dectris Corp., http://www.dectris.com/sites/dectris.html

The Princeton Plasma Physics Laboratory is operated
by Princeton University under contract
with the U.S. Department of Energy.

Information Services
Princeton Plasma Physics Laboratory
P.O. Box 451
Princeton, NJ 08543

Phone: 609-243-2245
Fax: 609-243-2751
e-mail: pppl_info@pppl.gov
Internet Address: http://www.pppl.gov